島根大学地球資源環境学研究報告　18, 1～10 ページ（1999 年 12 月）
Geoscience Rept. Shimane Univ., 18, p.1～10（1999）

Major and trace element analyses of Cretaceous sedimentary rocks from the Euisong block, Gyeongsang Supergroup, Korea

Barry Roser*, Hiroaki Ishiga*, Hyun-Koo Lee**, Kaori Dozen*** and Chikako Yamazaki*

Abstract

Cretaceous fluvial-lacustrine sedimentary rocks of the Gyeongsang Supergroup crop out extensively in southeast Korea. This report contains whole-rock XRF analyses of 81 sandstones, siltstones and shales from the Sindong and Hayang Groups in the Kumi-Euisong area of the Euisong block. Analyses include major elements, CO_2, LOI, and 11-16 trace elements. Sample suites, petrography and broad elemental variations are also outlined. SiO_2 concentrations vary from ~55 wt.% in the mudrocks to over 85% in the sandstones, due to sorting fractionation. Most elements are positively correlated with Al_2O_3, indicative of residence in the clay fractionation. A small group of elements (Na_2O, CaO, Ba, Sr) tend to decrease with increasing Al_2O_3, reflecting partial residence in feldspar and diagenetic enrichment in sandstones. Zr shows no trend, typical of zircon control. Scatter to high values for several other elements (Th, Ce, Ni, Cr, and Y) may also be influenced by heavy mineral concentration. More detailed interpretation of the data will be published elsewhere.

key words: Gyeongsang Supergroup, Cretaceous, sediments, geochemistry, Korea.

Introduction

Fluvial–lacustrine sedimentary rocks of the Cretaceous Gyeongsang Supergroup outcrop extensively in southeast Korea (Fig. 1). The sediments were deposited in the NNE–trending extensional intermontane Naktong Trough, which developed near the present margin of Korea during the Early Cretaceous (Yang and Chang 1987). The Gyeongsang sequence is divided into the Sindong, Hayang and Yuch'on Groups, in ascending order (Fig. 2). The Sindong Group (middle Early Cretaceous) is a 2000 to 3000m succession of sandstone, shale, conglomerate and marl. Paleocurrent data suggest derivation from a source to the WNW (Chang 1988). The Hayang Group (late Early Cretaceous) comprises a 1000 to 5000m sequence of shale and sandstone, with minor marl, conglomerate, and intrabasinal volcanics. The basin expanded eastward during Hayang deposition, and was cut into three smaller crustal blocks (Yongyang, Euisong, and Milyang) by movement along WNW-trending growth faults. In the southern Milyang block, the source of the Hayang Group is thought to lie to the east, under the present Japan Sea (Yang and Chang 1987). In the Euisong area, however, paleocurrents remain dominated by WNW directions (Chang, 1988) similar to those in the underlying Sindong Group. Throughout the basin, the Hayang Group is unconformably overlain by the complex Yuchon Group, which is dominated by abundant andesitic to rhyolitic volcanic rocks, and contains only minor volcaniclastic sediments.

This paper reports the whole-rock geochemistry of sandstones, siltstones and mudstones (shales) from a traverse across the Sindong Group and part of the Hayang Groups in the Euisong block. The samples were collected to determine basic geochemical variations and their cause, and geochemical parameters relating to provenance, tectonic setting and source weathering. The purpose of this paper is simply to present the data; interpretation of the results is given elsewhere (Roser et al. 2000). The sample suite reported here is intended to serve as a comparative baseline dataset for use in study of a second transect across the Milyang block, and of equivalent formations in western Japan.

Geological Outline and Sample Suites

The samples were collected between Kumi and Euisong, over an area of about 30x15 km (Fig. 1). Schematic stratigraphic sequence in the area is outlined

* Dept of Geoscience, Shimane University, 1060 Nishikawatsu, Matsue 690-8504, Japan
** Dept of Geology, Chungnam National University, Taejon 305-764, Korea
***Dept of Geosciences, Osaka City University, Osaka 558-8585, Japan

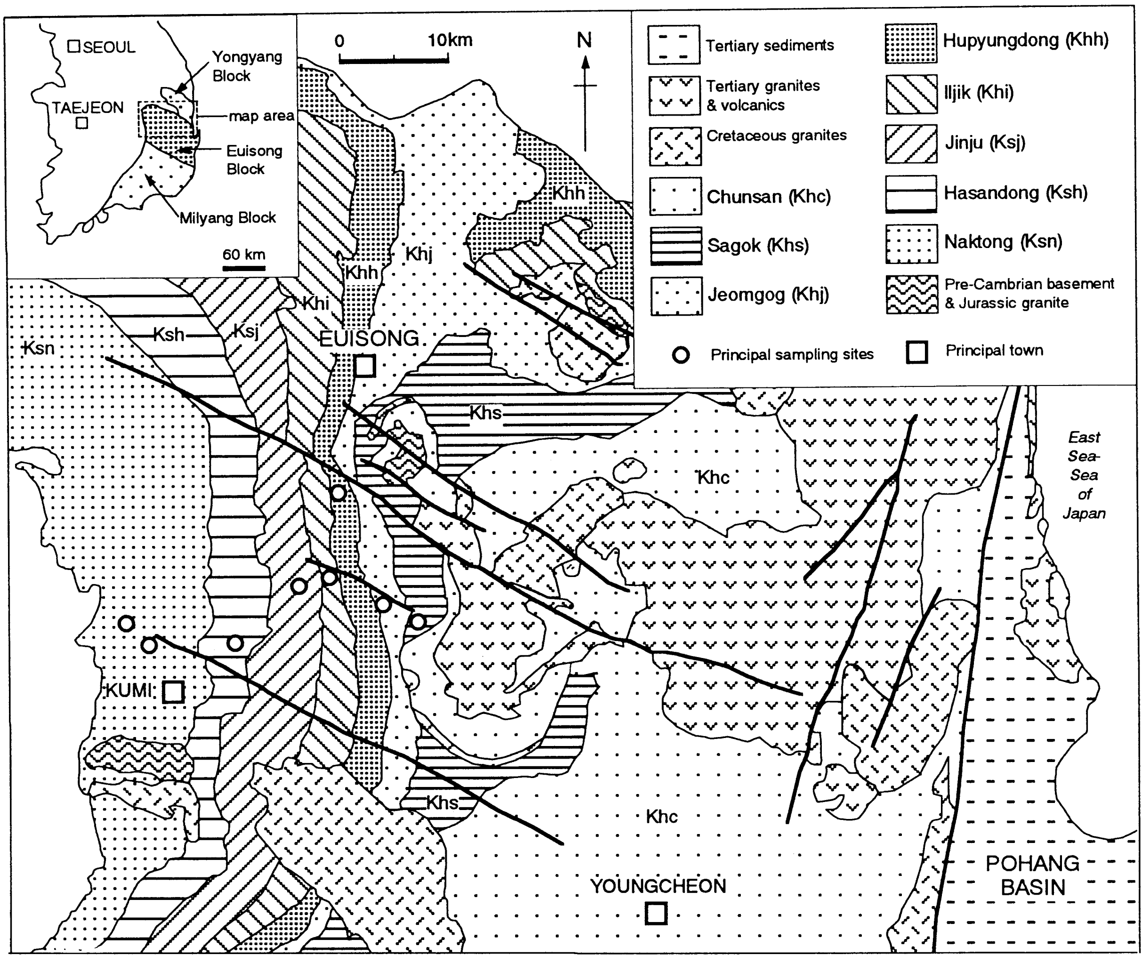

Fig. 1. Geology of the Gyeongsang Supergroup in the Kumi-Euisong area, Euisong block, showing locality and principal sampling sites. Inset: Korea, showing location of the main map, extent of the Gyeongsang Supergroup, and the Yongyang, Euisong and Milyang blocks. Figure from Roser et al. (2000).

in Fig. 2. Samples were taken mainly from clean roadside outcrops, and postdepositional weathering was absent or minimal. Sampling at individual outcrops was designed to span the full range of grain size present, to accommodate chemical fractionation resulting from mineralogical sorting. A total of 81 samples were collected and analysed, with 41 from the Sindong Group, and the remainder from the lower to middle formations of the Hayang Group. The Yuchon Group was not sampled. Stratigraphy, lithology, sample suites and petrography of the formations sampled are briefly outlined below, summarised from Roser et al. (2000). Sample numbers (in parentheses) refer to those listed in Tables 1 and 2. Those with alpha-numeric sample numbers are mainly sandstones, with a few siltstones and shales (collected by B.P.R.), whereas the 11xx-xx series samples are all shales collected by H.I. and K.D.

Sindong Group

The Sindong Group (Necomian) comprises the Naktong, Hasandong and Jinju Formations, in ascending order (Fig. 2). The Naktong Formation (12 samples) consists of alluvial fan and braided river pebble and cobble conglomerates, sandstone, siltstone, shale and marl (Choi 1986; Yang and Chang 1987; Son 1997). Beds at sites sampled included 2m thick matrix-supported cobble conglomerates containing coarse-medium channel sands (NK2-4), and 1-2 dm rhythmically bedded alternations of coarse- to medium -grained sandstones and subordinate mudrocks. Sandstones are arkosic, poorly to moderately sorted (NK5, 7) and usually massive (NK4), but occasionally show distinct plane lamination (NK6).

The Hasandong Formation (18 samples) includes sandstones, conglomerates and reddish and grey silty

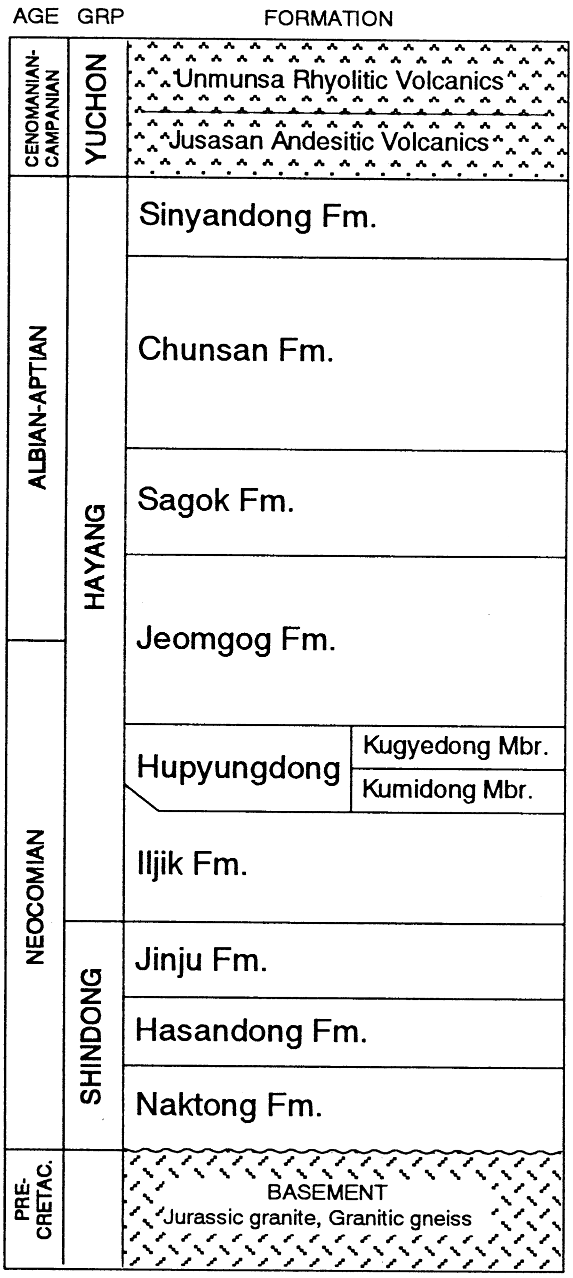

Fig. 2. Schematic stratigraphy of the Gyeongsang Supergroup in the Euisong block, after Son (1997).

shales, thought to have been deposited from meandering river systems (Son, 1997). Although the formation is partially distinguished in the field by incidence of reddish beds (Yang & Chang 1987) most sandstones collected here are pale grey, weakly laminated and graded medium-coarse sands (e.g. HA2, 7, 8), with muds comprising <2-10% of outcrop. Beds sampled ranged from 0.4 to 0.8m in thickness. Shale rip-up clasts present in some samples (e.g. HA8) were discarded prior to analysis.

Jinju Formation (11 samples) consists of fluvio-lacustrine sandstone, shale, and conglomerate (Son 1997). Red beds are generally lacking (Yang and Chang 1987). Sandstones collected here are mainly pale grey to pale brownish grey, moderately to well sorted, and fine or medium grained, although some coarser conglomeratic beds also occur. The sandstones sampled occur in 1-2 dm graded alternations with 10 cm grey shale interbeds. Weak lamination (CH2, 3, 6) and rip-up clasts (CH6, 7) are sometimes observed.

Hayang Group

Fluvial sediments of the Iljik Formation (8 samples) form the base of the Neocomian-Aptian Hayang Group in the study area. The two localities sampled consisted of rhythmic alternations of 1-10cm bedded pale brownish-grey sandstone and shale, in a ratio of 9 : 1. Sandstones at these sites were fine- to medium-grained, poorly or moderately sorted (IL2, 3), and sometimes showed weak grading (IL1).

The Hupyongdong Formation (conglomerate, sandstone and shale) is partially correlative with the Iljik Formation, and contains basal conglomerates where it directly overlies basement (Yang & Chang 1987). It is divided into the Kumidong and Kugyedong members (Fig. 2). Because the locality sampled here lies at the contact between these two members, only fine sandstones, siltstones and shales are present. All 17 samples analysed are distinctly coloured (red, maroon and purplish-red). Sandstones are typically well-sorted, very fine grained, and finely laminated (PA1, 2, 5). These occur in metre-thick beds separated by 2-3 m layers of fissile siltstone and shale, which become thicker upwards.

Strong colouration in the Hupyongdong Formation is succeeded by primarily grey to greenish-grey lacustrine sandstones and shales of the Jeomgog Formation (Son 1997). Ten samples were analysed, from two localities. The beds sampled were 1-10 dm bedded sandstone-shale alternations in which shale predominated. Sandstones (CG1-3) are calcareous, well sorted, fine- to medium-grained, and plane laminated.

The uppermost unit sampled in this study is the Sagok Formation (5 samples), which is a mud-dominated flood plain unit (Son 1997). The main locality sampled consisted of shale alternating with subordinate 80cm-thick purplish-grey, weakly laminated fine-grained sandstone beds (SA1, 2).

Petrography

Petrographic studies (Yun et al. 1993 ; Lee and Lee 1998) and representative thin sections in this study show that Sindong and Hayang sandstones are relatively quartz-rich feldspathic wackes. Lithic fragments are rare, but matrix and cement contents are significant (Yun et al. 1993), suggesting some labile lithic fragments have been destroyed by post-depositional processes Quartz and feldspar are typically angular to subangular. Feldspar includes abundant sodic plagioclase, and K-feldspar often exhibits microcline twinning, and perthite and braid perthite microtextures. All feldspar shows alteration, with pools of calcite and flecks of sericite. Accessory minerals include biotite, muscovite, amphibole and epidote. Identifiable lithic fragments include gneissic and schistose metamorphics, quartz-feldspar aggregates and fine-grained sedimentary rock fragments. Volcanic rock fragments, which are abundant in Hayang Group sandstones in the Milyang block (Noh and Park 1990, Lee and Jun 1995 ; cited in Lee and Lee 1998), are virtually absent in this sample suite.

Petrographic information loss from extensive matrix development is compounded by almost ubiquitous presence of sparry and granular carbonate cement. In some samples from the Hayang Group, such cement surrounds and isolates subrounded detrital phases, and may near 50 modal per cent. This precludes systematic point-counting of the samples collected. Albitisation of feldspar is extensive in the Gyeongsang sediments, as shown by Lee and Lee (1998). Diagenetic modification is thus well advanced, and has substantially modified both petrographic and chemical compositions.

Analytical Methods

All samples were analysed by XRF, using a Rigaku RIX-2000 XRF at Shimane University. This instrument is equipped with an Rh-anode X-ray tube. All analyses were carried out on an anhydrous basis, using the ignited material from loss on ignition (LOI) determinations. LOI was measured by weight loss in 5-6 g of oven dried (110℃) sample after ignition for two hours in ceramic crucibles at 1000℃. Sample preparation and analysis methods differed between the 11xx-xx series shale samples (analysts K.D and S.Y.) and the sandstone-dominated alpha numeric sample suite (analyst B.P.R.).

11xx-xx series

About 20 g washed and dried sample chip was manually crushed in a tungsten carbide pestle and mortar, and then ground in an automatic agate pestle and mortar grinder. The powders were then oven-dried at 110℃ for 24 hours prior to LOI determination. Major and trace elements were determined on fused glass beads prepared in an automatic bead sampler, using commercial lithium tetraborate flux and a sample : flux ratio of 1 : 5. For major elements the method is essentially that of Norrish and Hutton (1969). Trace element analyses used standard peak over background methods, utilising calibration lines constructed from data for standard rocks issued by the Geological Survey of Japan (G.S.J.) and the United States Geological Survey (U.S.G.S.). Instrumental drift during analysis was monitored by repeat analysis of U.S.G.S. standard SCo-1.

Alpha numeric sample suite

Fresh sample chip <10 mm in diameter was produced by splitting in a manual rock trimmer, with any chip containing exterior surfaces, veins or rip-up clasts being discarded. Sample chip was washed repeatedly in deionised water, oven-dried, and crushed for 30-60 seconds in a tungsten-carbide ring mill. Sample weights ranged from 70 g in the shales and siltstones to approximately 200 g in the sandstones. Previous work (Roser et al. 1998) has shown that the crushing times used produce powders finer than agate grinding, with no significant contamination other than for Co, which was not analysed. The powders were oven-dried at 110℃ for 24 hours prior to LOI determination.

All analyses were carried out on glass beads prepared in an automatic bead sampler, using commercial alkali flux comprising 80% lithium tetraborate and 20% lithium metaborate, with a sample to flux ratio of 1 : 2. Analytical methods and instrumental conditions for these analyses follow those described by Kimura & Yamada (1996). The 1 : 2 method used for this group of samples allows determination of several additional elements (Th, Ce, Ga, As, Pb), and also offers greater precision over the 1 : 5 trace element data due to greater peak/background

Table 1 Major and trace element analyses of sandstones, siltstones and shales from the Sindong Group, Euisong district. Major elements wt%, trace elements ppm (hydrous basis).

SaNr	Pstn	LITH	SiO_2	TiO_2	Al2O3	Fe_2O_3	MnO	MgO	CaO	Na_2O	K_2O	P_2O_5	CO_2	REST	SUM	As	Ba	Ce	Cr	Cu	Ga	Nb	Ni	Pb	Rb	Sr	Th	V	Y	Zn	Zr
SINDONG GROUP																															
Naktong																															
NK2	L	MS	74.15	0.20	10.12	2.29	0.05	1.27	3.64	1.45	2.82	0.05	2.65	1.39	100.08	5	643	29	74	6	12	7	25	14	90	187	5.3	21	16	28	104
NK3	L	VCS	74.07	0.28	11.81	2.01	0.03	1.09	2.19	2.01	3.26	0.06	1.56	1.34	99.71	9	751	46	25	7	15	7	19	19	101	237	8.2	29	14	30	128
NK4	L	FS	76.83	0.27	9.51	1.99	0.04	1.15	2.64	1.49	2.34	0.06	1.95	1.32	99.59	8	530	47	93	8	12	8	26	15	79	156	7.4	31	13	27	156
NK8	L	MS	75.37	0.29	8.84	2.18	0.05	1.50	3.88	1.77	1.66	0.06	2.73	1.47	99.80	2	341	43	96	<2	10	9	43	9	52	149	5.0	34	14	17	160
1102-1a	L	Mst	64.35	0.85	17.80	4.04	0.03	2.88	0.82	0.15	5.05	0.10	-	4.25	100.32	-	758	-	115	34	-	16	35	-	255	30	-	107	21	77	180
1102-1b	L	Mst	62.25	0.93	19.23	4.77	0.02	2.60	0.48	0.13	5.25	0.15	-	4.63	100.44	-	773	-	109	39	-	16	43	-	243	56	-	129	27	116	167
NK5	U	MS	78.56	0.17	8.75	1.68	0.04	1.15	2.56	1.88	1.82	0.05	1.74	1.23	99.63	3	374	35	47	7	10	7	37	16	62	164	4.9	20	11	27	81
NK6	U	FS	59.23	0.41	9.07	1.98	0.20	1.24	12.58	1.27	2.25	0.10	9.39	1.96	99.68	4	480	72	78	14	11	13	34	13	78	156	9.4	49	22	33	243
NK7	U	MS	78.52	0.19	8.46	1.61	0.05	1.06	2.87	1.80	1.67	0.05	1.91	1.33	99.52	3	336	30	56	7	9	7	33	15	56	169	4.6	21	13	24	91
1102-2a	U	Mst	62.39	0.99	17.92	4.79	0.04	2.86	0.71	0.83	4.48	0.18	-	4.64	99.83	-	770	-	141	35	-	17	61	-	199	59	-	106	31	85	234
1102-2b	U	Mst	58.30	0.69	13.20	5.44	0.06	2.74	6.72	0.75	3.06	0.16	4.73	3.74	99.59	-	547	-	128	29	-	9	73	-	138	125	-	70	32	83	184
1102-2c	U	Mst	55.76	0.77	17.23	5.58	0.06	3.01	4.75	0.24	4.58	0.14	3.20	4.86	100.18	-	688	-	117	36	-	13	63	-	216	87	-	90	32	91	140
Hasandong																															
HAI	L	CS	76.18	0.30	10.40	1.94	0.03	1.49	1.67	2.60	2.42	0.06	1.25	1.19	99.53	<2	763	56	51	16	12	8	19	16	76	276	10.4	35	13	22	110
HA2	L	MS	72.00	0.36	10.45	2.28	0.04	1.45	3.67	0.69	2.77	0.07	4.65	1.40	99.83	35	353	74	103	8	14	11	47	15	91	155	9.2	43	16	15	209
HA3	L	FS	75.87	0.30	9.18	2.41	0.05	1.47	3.05	1.86	1.69	0.06	2.65	1.23	99.82	5	303	53	128	5	11	9	39	19	59	204	8.4	37	15	30	131
HA4	L	FS	75.91	0.34	8.87	2.12	0.05	1.32	3.69	1.89	1.69	0.06	2.58	1.39	99.91	2	364	63	93	7	10	9	30	15	57	194	7.4	35	16	27	210
1102-4a	L	Mst	61.36	0.56	14.11	3.81	0.02	1.92	0.85	1.16	3.28	0.16	-	10.14	97.37	-	710	-	130	12	-	13	93	-	111	114	-	75	19	18	222
HA6	M	FS	76.68	0.25	10.57	1.94	0.04	0.82	2.09	2.26	1.98	0.04	1.39	1.37	99.43	2	331	37	19	5	13	7	10	7	77	191	7.1	23	14	27	104
HA7	M	MS	77.13	0.21	11.05	1.43	0.03	0.69	1.50	2.64	2.46	0.04	1.14	1.16	99.48	<2	467	33	12	6	13	7	8	19	88	231	7.3	33	11	22	91
HA8	M	MS	77.00	0.25	10.85	2.05	0.04	1.16	1.42	2.62	2.04	0.05	0.93	1.36	99.77	2	405	48	18	3	13	8	9	13	77	253	7.5	27	13	34	141
HA8A	M	FS	72.87	0.53	11.79	3.30	0.04	1.51	2.18	1.79	2.73	0.10	1.18	1.59	99.61	3	595	112	37	5	16	14	17	8	110	198	18.4	58	24	48	388
HA9	M	VFS	63.22	0.77	14.76	5.82	0.06	2.76	3.13	1.07	3.71	0.15	2.16	2.49	100.10	3	700	88	71	21	23	20	38	51	170	140	16.9	106	29	93	231
HA10	M	VFS	72.32	0.40	12.29	2.56	0.05	2.07	2.17	1.67	2.89	0.06	1.32	1.93	99.73	5	531	43	38	58	16	12	20	7	123	170	7.9	78	15	61	125
HA11	M	MS	66.93	0.38	11.37	2.26	0.06	1.47	6.78	1.54	2.93	0.07	4.48	1.92	100.19	4	810	48	35	<2	13	11	19	11	116	186	8.1	72	17	38	153
1102-7a	M	Mst	61.31	0.79	15.82	6.44	0.06	2.80	2.66	1.13	3.72	0.14	-	4.97	99.84	-	563	-	74	27	-	12	32	-	179	136	-	92	28	99	200
1102-7b	M	Mst	58.33	0.87	18.64	8.12	0.04	3.14	0.63	0.73	4.66	0.12	-	4.38	99.66	-	788	-	88	73	-	13	40	-	257	67	-	85	17	104	153
1102-7c	M	Mst	66.62	0.77	14.51	5.44	0.04	2.35	1.46	1.18	3.95	0.12	-	2.93	99.37	-	614	-	71	3	-	13	30	-	197	113	-	83	21	75	243
1102-7d	M	Mst	57.44	0.62	15.14	4.72	0.06	2.77	6.51	0.57	4.46	0.19	3.99	3.77	100.24	-	646	-	62	63	-	11	27	-	196	174	-	65	34	76	178
HA5	U	FS	72.97	0.30	11.00	2.34	0.06	0.46	4.04	0.04	3.18	0.05	3.18	1.94	99.56	12	308	51	19	15	13	12	11	3	106	23	7.1	35	14	13	131
1102-5a	U	Mst	52.94	0.94	18.79	3.56	0.08	2.42	4.45	0.04	5.68	0.18	6.33	5.65	101.06	-	430	-	151	25	-	20	59	-	198	107	-	115	50	25	165
Chinju																															
CH1	L	MS	77.23	0.37	11.26	1.88	0.03	0.78	0.90	2.62	2.80	0.06	0.76	0.88	99.57	3	699	75	23	5	14	11	9	23	103	231	13.1	44	17	30	137
CH2	L	MS	73.69	0.83	12.51	3.00	0.04	1.32	0.74	2.20	3.22	0.12	0.41	1.39	99.47	6	875	185	44	2	17	20	16	14	116	191	26.2	71	30	35	616
CH3	L	FS	73.39	0.42	11.37	3.06	0.05	1.58	2.08	1.91	2.61	0.08	1.49	1.59	99.63	8	720	71	84	11	16	12	50	17	93	148	10.1	58	18	52	220
1102-6a	L	Mst	55.13	1.15	24.26	4.78	0.05	2.70	0.27	0.90	6.67	0.10	-	5.22	101.23	-	1232	-	126	43	-	23	22	-	290	70	-	128	34	70	224
1102-6b	L	Mst	57.53	1.19	22.51	4.99	0.04	3.10	0.26	0.89	5.97	0.15	-	4.32	100.95	-	1204	-	112	25	-	24	38	-	231	68	-	137	38	92	290
CH4	M	CS	75.15	0.19	9.88	1.76	0.04	0.71	3.10	2.60	2.41	0.06	2.86	1.01	99.77	7	560	41	28	4	11	5	14	20	73	320	5.9	28	12	21	101
CH5	M	FS	70.30	0.30	9.81	2.70	0.08	0.81	5.25	2.21	2.30	0.08	4.55	1.40	99.79	6	625	45	43	6	13	8	16	21	70	303	7.9	36	16	25	143
CH6	M	MS	78.56	0.25	10.12	1.44	0.03	0.62	1.76	3.07	1.51	0.05	1.18	0.94	99.53	3	281	51	14	4	12	7	8	21	57	284	6.8	27	12	24	128
CH7	M	FS	67.19	0.45	11.91	3.25	0.10	1.48	5.09	2.21	2.73	0.10	3.71	1.62	99.84	2	629	80	39	11	16	11	21	27	97	295	11.9	49	30	52	246
1103-2a	M	Mst	61.71	0.83	16.16	6.57	0.05	3.09	1.49	1.26	3.57	0.15	-	4.71	99.59	-	593	-	85	31	-	15	42	-	178	115	-	93	29	121	200
1103-2b	M	Mst	58.96	0.81	17.25	6.80	0.05	3.25	1.87	1.01	3.94	0.15	-	5.58	99.67	-	648	-	90	41	-	14	42	-	199	108	-	101	28	110	166

Notes: Pstn=stratigraphic position (L=Lower; M=Middle; U=Upper; nd=not differentiated). LITH=lithology (VCS=very coarse sandstone; CS=coarse sst; MS=medium sst; FS=fine sst; VFS=very fine sst; Zst=siltstone; Mst=mudstone/shale). REST=LOI-CO_2. Where CO_2 was not determined, REST=LOI. For elemental data," -" equals not determined.

Table 2 Major and trace element analyses of sandstones, siltstones and mudstones from the Hayang Group, Euisong district. Major elements wt%, trace elements ppm (hydrous basis).

SaNr	Pstn	LITH	SiO_2	TiO_2	Al2O3	Fe_2O_3	MnO	MgO	CaO	Na_2O	K_2O	P_2O_5	CO_2	REST	SUM	As	Ba	Ce	Cr	Cu	Ga	Nb	Ni	Pb	Rb	Sr	Th	V	Y	Zn	Zr
HAYANG GROUP																															
Ilchik																															
IL1	L	FS	73.97	0.28	10.94	1.61	0.07	0.40	3.45	4.09	1.62	0.05	2.23	0.97	99.68	2	529	87	15	10	10	8	6	7	64	173	16.7	28	27	16	240
IL2	L	FS	70.86	0.58	14.25	3.66	0.04	1.50	0.39	4.29	2.24	0.11	0.05	1.63	99.60	3	291	185	31	<2	19	12	14	8	96	170	35.6	64	40	53	596
IL3	L	MS	79.92	0.15	10.62	0.89	0.05	0.28	0.93	4.09	1.65	0.05	0.48	0.59	99.70	2	679	37	8	11	10	6	5	8	63	158	5.2	13	14	12	102
IL4	L	MS	77.80	0.22	10.26	1.51	0.04	0.67	2.21	3.08	1.66	0.04	1.52	1.03	100.04	4	302	38	11	0	11	7	8	20	60	275	6.3	22	11	11	94
IL5	L	Mst	61.78	0.76	15.24	6.30	0.07	3.01	2.64	1.55	3.31	0.15	1.61	3.32	99.74	7	637	92	79	21	20	19	45	31	142	149	17.1	108	37	107	237
IL6	L	VFS	59.93	0.69	14.18	6.27	0.08	3.13	4.87	1.47	2.92	0.14	3.21	3.23	100.12	8	602	91	70	16	19	19	37	22	127	183	15.3	109	34	94	220
1103-3a	L	Mst	62.05	0.76	18.65	5.00	0.03	2.93	0.54	3.26	3.62	0.16	-	3.03	100.03	-	391	-	49	3	-	8	21	-	156	151	-	76	51	86	753
1103-3b	L	Mst	57.19	0.90	21.34	6.54	0.02	2.96	0.52	1.84	5.45	0.16	-	3.75	100.67	-	485	-	66	12	-	17	25	-	273	87	-	86	30	85	247
Hupyungdong																															
Paeksodong & Kumidong Members																															
PA1	nd	VFS	79.43	0.29	8.63	1.67	0.04	0.34	2.51	2.94	1.30	0.05	1.74	0.84	99.78	2	2542	14	25	7	9	8	9	7	47	127	6.6	36	13	20	154
PA2	nd	VFS	78.94	0.36	9.43	1.85	0.06	0.54	1.81	3.05	1.48	0.05	1.21	0.93	99.71	3	889	61	25	8	10	8	12	8	55	120	8.0	33	16	28	271
PA3	nd	VFS	85.32	0.16	8.14	0.75	0.06	0.16	0.16	3.38	0.83	0.04	0.02	0.52	99.54	2	159	27	14	36	7	6	6	5	30	65	3.3	18	9	10	88
PA4	nd	MS	69.68	0.09	10.44	0.68	0.09	0.21	6.87	3.95	1.64	0.04	4.97	0.76	99.42	2	430	27	5	55	10	4	5	5	44	173	3.3	8	13	12	63
PA5	nd	FS	78.81	0.14	11.37	1.18	0.03	0.48	0.61	4.38	1.49	0.04	0.33	0.89	99.75	2	233	20	13	37	13	6	18	7	45	86	3.5	50	12	24	75
PA6	nd	VFS	60.38	0.47	11.44	2.14	0.15	1.43	10.22	2.26	2.10	0.10	7.39	2.02	100.10	2	275	62	38	30	13	10	18	13	77	187	9.1	68	21	43	186
PA7	nd	Zst	61.47	0.55	12.95	4.02	0.07	2.67	6.18	3.18	2.05	0.10	4.36	2.25	99.85	3	1459	56	60	20	17	14	25	14	81	229	10.0	89	21	75	199
KM2	nd	Zst	61.87	0.59	13.27	3.98	0.08	2.17	6.17	3.58	1.73	0.12	4.20	2.25	100.01	<2	436	33	62	9	17	16	27	5	71	170	3.9	95	29	70	258
KM1	nd	VFS	61.13	0.54	13.08	3.71	0.08	1.96	7.05	3.15	2.07	0.10	4.90	2.37	100.14	4	525	86	56	33	17	16	28	14	86	185	12.6	86	25	67	228
KM3	nd	Zst	69.49	0.50	10.44	2.56	0.10	0.92	5.80	3.04	1.75	0.06	4.08	1.39	100.13	4	1609	62	47	8	11	10	16	13	63	196	9.0	58	23	26	301
KM4	nd	VFS	61.34	0.56	12.28	3.74	0.09	2.08	7.55	1.96	2.46	0.14	5.31	2.45	99.96	3	772	70	45	14	15	12	24	16	93	188	9.8	78	24	64	209
1103-4a	nd	Mst	69.14	0.73	14.13	4.42	0.02	1.37	1.05	2.14	3.42	0.08	-	2.93	99.43	-	319	-	59	9	-	9	27	-	148	83	-	62	14	52	204
1103-4b	nd	Mst	66.92	0.69	11.31	3.43	0.08	0.97	5.40	2.43	2.38	0.08	3.75	1.76	99.20	-	279	-	68	8	-	8	19	-	90	124	-	60	36	39	548
1103-4c	nd	Mst	70.45	0.67	14.42	3.61	0.01	1.48	0.50	2.39	3.13	0.10	-	2.65	99.41	-	452	-	61	10	-	7	28	-	129	90	-	64	21	59	220
1103-4d	nd	Mst	58.36	0.97	21.58	4.05	0.01	2.60	0.45	1.06	5.82	0.14	-	5.68	100.72	-	450	-	103	46	-	17	27	-	226	60	-	206	57	86	183
1103-4e	nd	Mst	70.71	0.58	12.12	3.53	0.03	0.70	2.82	2.71	2.48	0.08	-	3.52	99.28	-	551	-	52	3	-	6	23	-	96	122	-	53	23	46	269
1103-4f	nd	Mst	65.01	0.63	13.01	3.89	0.05	1.77	4.82	2.42	2.60	0.13	3.21	2.45	99.99	-	434	-	58	10	-	10	25	-	109	120	-	57	27	62	207
Chomgok																															
CG1	nd	VFS	57.02	0.51	11.76	4.56	0.09	3.11	9.24	2.26	2.01	0.13	7.08	2.42	100.19	3	265	63	54	194	15	15	30	4	77	161	13.6	73	26	77	130
CG2	nd	Zst	58.73	0.49	10.76	3.59	0.14	2.13	10.86	3.19	1.43	0.12	8.62	0.34	100.40	32	214	77	42	27	11	14	28	24	53	173	11.9	67	25	44	137
CG3	nd	VFS	56.60	0.50	13.79	4.88	0.09	2.96	6.63	3.08	3.78	0.17	3.35	4.28	100.11	2	796	68	66	21	19	7	38	20	136	505	14.2	98	23	76	171
CG4	nd	Zst	51.01	0.64	14.37	5.88	0.13	3.70	8.19	3.80	3.19	0.22	6.14	2.58	99.85	2	383	74	62	14	19	10	44	11	110	520	13.6	123	26	88	166
CG5	nd	Zst	54.50	0.55	14.27	5.62	0.09	4.27	5.77	3.09	4.20	0.13	4.72	2.60	99.81	3	575	54	63	18	18	9	48	13	131	403	11.3	96	22	74	139
1103-5a	nd	Mst	53.89	0.61	14.26	5.63	0.08	3.34	8.10	1.75	3.02	0.16	5.99	3.29	100.12	-	317	-	57	18	-	8	32	-	113	120	-	76	31	110	117
1103-5b	nd	Mst	47.24	0.39	12.15	2.93	0.14	2.35	15.58	3.08	1.69	0.23	11.69	2.37	99.84	-	523	-	30	119	-	5	13	-	46	572	-	32	37	49	115
1103-5c	nd	Mst	49.99	0.50	14.32	3.66	0.09	2.78	11.20	2.34	3.20	0.16	8.42	3.63	100.29	-	210	-	52	25	-	6	24	-	104	222	-	138	24	82	97
1103-6a	nd	Mst	51.93	0.67	16.36	6.56	0.08	4.22	5.36	2.29	4.96	0.18	4.10	3.52	100.23	-	423	-	66	8	-	8	41	-	186	272	-	107	27	85	148
1103-9	nd	Mst	51.28	0.58	14.04	5.12	0.08	3.38	8.88	1.98	3.65	0.15	6.58	2.92	98.64	-	470	-	66	31	-	5	27	-	129	595	-	75	31	70	192
Sagok																															
SA1	nd	VFS	68.19	0.32	11.35	2.26	0.07	2.02	5.28	2.45	2.57	0.11	4.34	0.77	99.73	3	757	53	32	25	15	9	20	16	90	238	10.1	46	16	59	166
SA2	nd	FS	68.38	0.27	10.30	1.70	0.10	1.46	6.74	2.50	2.66	0.09	5.57	0.10	99.87	2	757	43	26	21	13	7	14	18	79	244	8.1	36	16	41	135
SA3	nd	Mst	58.42	0.54	9.80	2.06	0.14	1.75	12.32	2.94	1.21	0.16	8.95	1.67	99.96	3	461	63	55	26	9	11	20	13	42	253	8.5	59	24	34	176
SA4	nd	FS	66.92	0.31	10.49	1.63	0.07	2.45	4.72	3.52	2.67	0.06	6.36	1.04	100.24	6	416	50	62	<2	12	8	15	11	66	174	5.5	48	14	15	171
1103-7a	nd	Mst	53.65	0.72	16.67	6.63	0.06	3.46	5.51	1.62	4.53	0.19	3.88	3.49	100.41	-	388	-	77	18	-	8	37	-	181	117	-	98	25	100	133

Notes: As in Table 1.

intensities. Analysis of a number of elements in several sandstones by both the 1 : 2 and 1 : 5 methods showed that comparability was excellent (better than 5% relative for most elements). Calibration lines were again constructed from data from beads of a similar suite of G.S.J. and U.S.G.S. standard rocks as used above, and instrumental drift monitored by repeat analysis of G.S.J. standards JB-1a and JG-1a.

Carbon dioxide determinations

CO_2 in oven-dried hydrous powders was determined (B.P.R., K.D. and C.Y.) to permit calculation of sample carbonate content, and thus allow derivation of detrital CaO (CaO*), as used in the Chemical Index of Alteration (C.I.A.) of Nesbitt and Young (1982, 1984). Analyses were carried out by gas chromatography, using a Fisons EA 1108 elemental analyser at Shimane University, calibrated using BBOT organic standard [2.5-Bis - (5-tert-butyl-benzoxacol-2-yl) - thiothiophen: FISONS Instruments].

In this method total carbon (C_{TOT}) is first measured, using approximately 10 mg of sample. Duplicate analysis of several samples showed agreement within 3% error (coefficient of variation). Total sulphur and nitrogen were also sought in the analysis, but contents were not detectable or were negligible. Organic carbon (C_{org}) was then measured in a second run, after dropwise treatment of the sample with 1M HCl to remove carbonate. Acid treatment of the samples was repeated until effervescence ceased, and the samples subsequently dried at 110°C for 30 minutes prior to gas chromatographic analysis. Inorganic carbon (carbon in $CaCO_3$) is derived from subtraction of C_{org} from C_{TOT}, and is then recalculated to CO_2.

Initial data derived by this method slightly overestimated $CaCO_3$, leading to small negative values for CaO* in many samples. To resolve this anomaly, a subset of 13 samples spanning the full range of CO_2 observed was also analysed by conventional Leco techniques by the Analytical Facility, Victoria University of Wellington. These results showed a slight calibration bias (+10-11% relative) toward higher values in the gas chromatograph analyses, which was corrected using the Leco data in a secondary calibration. This removed the negative CaO* values. Subsequent analytical runs also included subsets of the Leco-analysed samples to allow secondary calibration in each sample set.

Results

Results for major and trace elements are listed in Table 1 (Sindong Group) and Table 2 (Hayang Group), by formation. The data are listed on a hydrous basis. Lithology was estimated visually, using a hand lens and grain size comparator.

Elemental abundances vary considerably, depending largely on lithology and carbonate content (Tables 1 & 2), as shown by example variation diagrams plotted against Al_2O_3 (Figs 3 & 4). Anhydrous SiO_2 contents vary between ~55 wt.% in the mudrocks and >85% in the sandstones (Fig. 3a). Differentiation between the two lithotypes induced by sorting fractionation is reasonably clear, with all sandstones containing <15% Al_2O_3. However, many of the mudrocks scatter below an idealised detrital trend (DT) to lower SiO_2 values than expected, and some overlap occurs between the two lithotypes. A number of other major elements (TiO_2, Fe_2O_3T, MgO, and P_2O_5) display similar patterns to K_2O (Fig. 3b), with increasing abundances with increasing Al_2O_3, suggestive of residence in the clay fraction. Trends resulting from sorting fractionation (arrowed) intersect the Al_2O_3 axis at ~6%, rather than following a silica dilution trend (SDL) from the most aluminous sample to the origin. This reflects abundances of detrital feldspar and lithic fragments, rather than a simple quartz-clay unmixing system. In contrast, the scatter plot for Na_2O (Fig. 3c), shows the reverse trend, with generally higher abundances in sandstones than in the mudrocks. Considerable scatter occurs, attributable to varying sodic feldspar contents and extent of diagenesis. In general, Hayang samples of both lithotypes are more sodic than Sindong equivalents, suggesting more extensive albitisation (Roser et al. 2000). CaO contents vary considerably, with values nearing 20 wt.% (Fig. 3d), reflecting variable carbonate cement contents. Dilution effects from this component account for the distribution of data below the detrital trend on the SiO_2 plot, and for much of the scatter in elements positively correlated with Al_2O_3, such as K_2O.

Trace element contents show equally wide variation. A large group of elements including Rb (Fig. 4a) Ce, Cr, Ga, Nb, Ni, Th, V, Y, and Zn are positively correlated with Al_2O_3, with marked sorting fractionation between sandstones and mudrocks. Although the

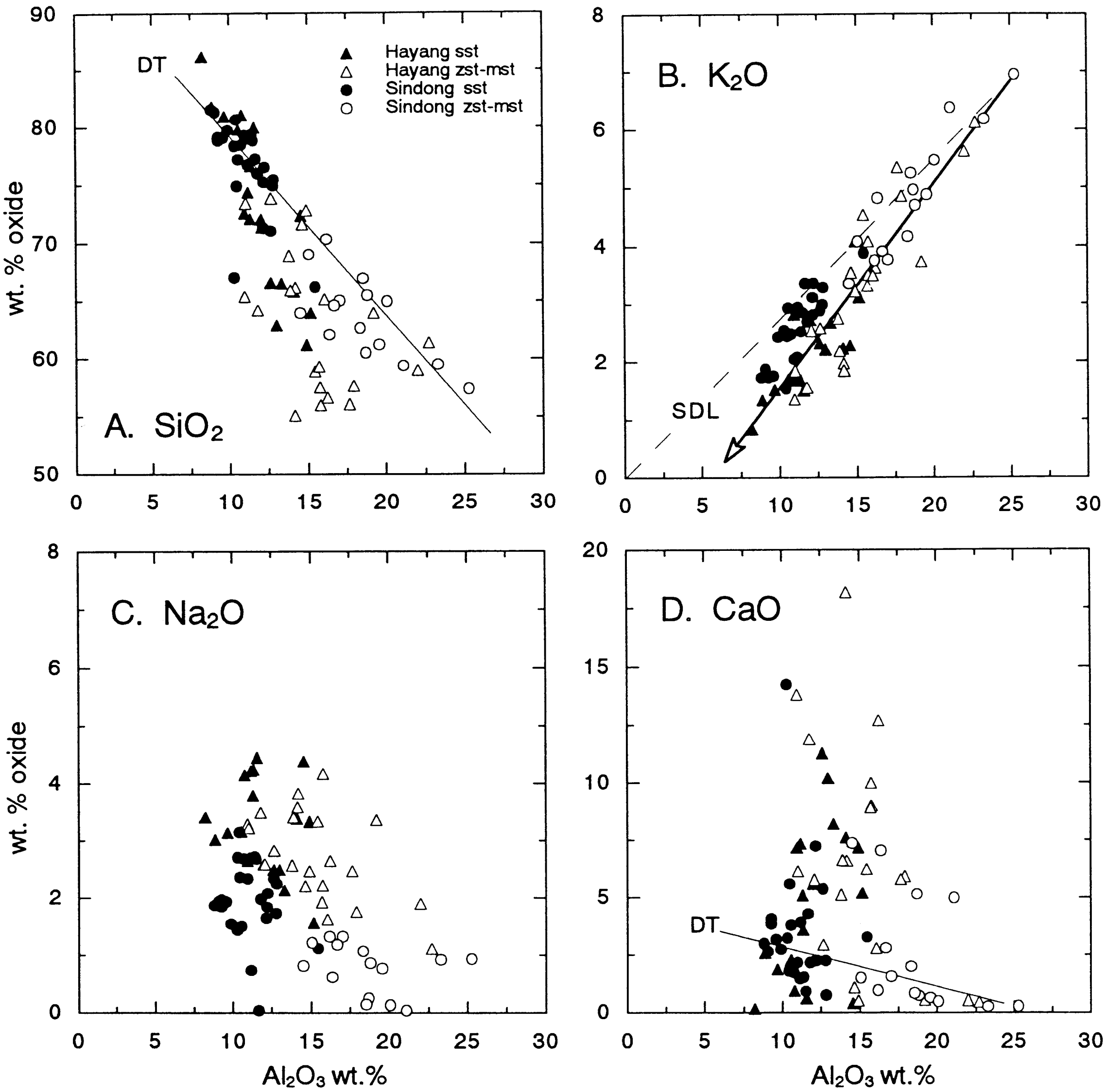

Fig. 3. Example oxide-Al_2O_3 variation diagrams, plotted on an anhydrous normalised basis. Solid line DT=detrital trend ; dashed line SDL (Fig. 3b) is a silica dilution trend from the most aluminous sample. Arrowed line on the K_2O plot illustrates the sorting fractionation trend. Sst=sandstone ; zst -mst=siltstones and shales.

strength of the trends vary, most intersect the Al_2O_3 axis between 5 and 10 wt.%, similar to the positively correlated major elements, indicative of primary residence in the clay fractionation. Some samples scatter to higher values for a few elements (e.g. Th, Ce, Ni, Cr, Y), suggesting partial residence in heavy mineral or ferromagnesian minerals, and sporadic enrichment of these phases.

Three other elements (Ba, Sr and Zr), however, display less consistent relationships with Al_2O_3 content. Barium contents are generally <1000 ppm, and abundances in sandstones and mudrocks overlap completely (Fig. 4b). This probably reflects residence in both the feldspar and clay fractions, although variable diagenesis may also be a factor. Isolated high values in mudrocks may also be due to presence of a Ba-rich phase such as barite, although this has not been confirmed. Strontium levels in sandstones are generally higher than in mudrocks, although both lithotypes show wide variation (Fig. 4c). Although this element is closely linked geochemically with Ca, their scatter plots differ, suggesting that Sr contents are not controlled by abundance of carbonate cement. The pattern of decreasing Sr with increasing Al_2O_3 is more similar to that of Na_2O, implying detrital feldspar control. Zirconium contents also show no relation with Al_2O_3 (Fig. 4d), with some scatter to very high values

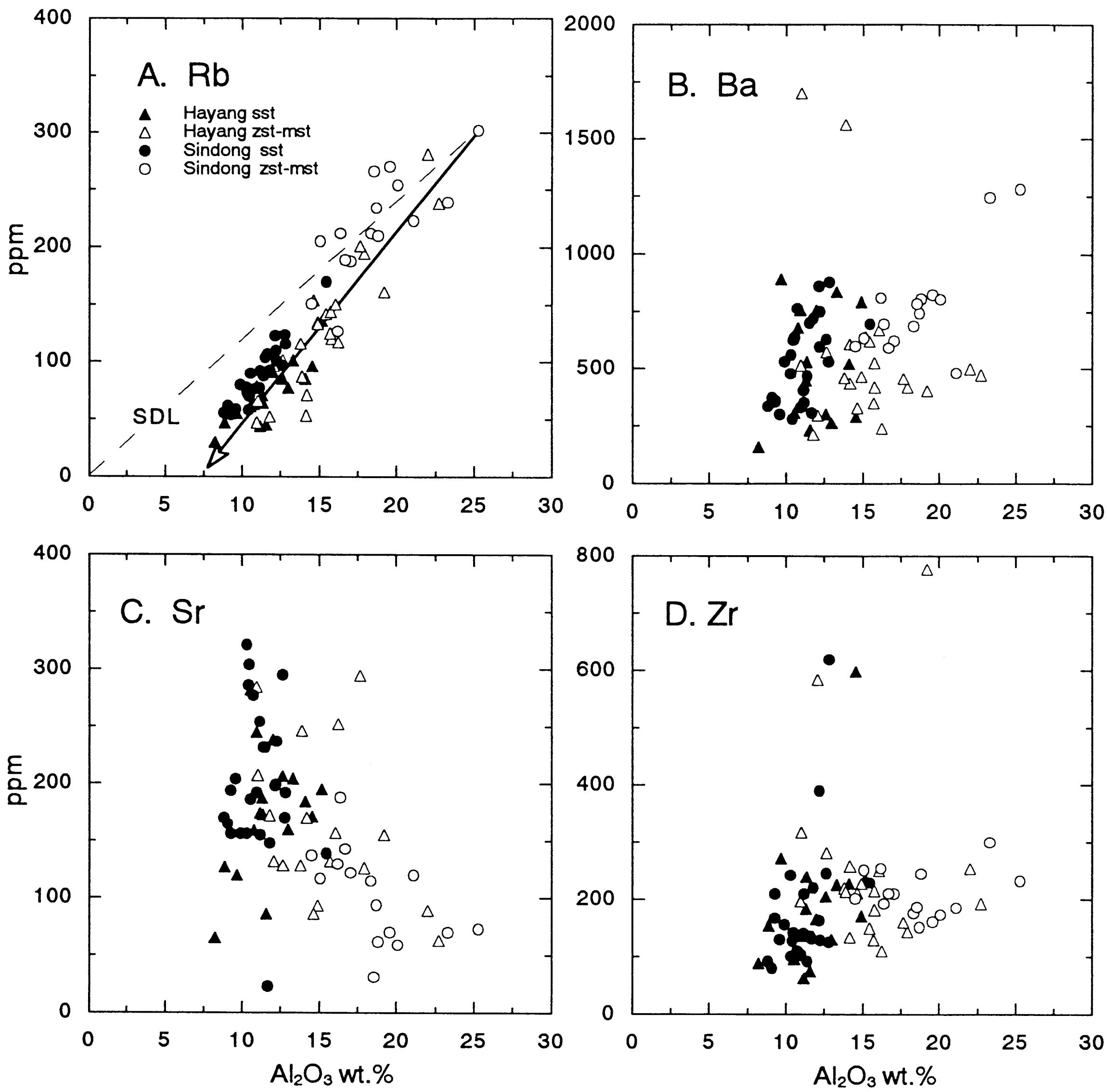

Fig. 4. Example trace element-Al_2O_3 variation diagrams, plotted on an anhydrous normalised basis. Symbols and lines as in Fig. 3.

in the range 10-15% Al_2O_3. This pattern is typical of primary residence in zircons. Several other elements (As, Cu, Pb) show little systematic variation in abundances, probable due to residence in multiple phases and variable diagenetic redistribution.

Acknowledgements

Our thanks to Y. Sawada and Y. Sampei of Shimane University for access to XRF and carbon analysis facilities, respectively, and to H.S. Yun and several members of the Geology departments of Chungsam and Pusan National Universities for assistance with field logistics. This work was supported by grants-in-aid 07045015 (S. Iizumi) and 08640571 (B.P. Roser) from the Japanese Ministry of Education, Culture and Science, and by the Basic Science Research Program of the Ministry of Education, Korea (BSRI-97-5419 ; H.K. Lee).

References

Chang, K.-H. 1988. Cretaceous stratigraphy and paleocurrent analysis of Kyongsang Basin, Korea. *Journal of the Geological Society of Korea,* 24, 194-205.

Choi, H.I., 1986. Fluvial plain/lacustrine facies transition in the Cretaceous Shindong Group, south coast of Korea. *Sedimentary Geology,* 48, 295-320.

Kimura, J.-I. and Yamada, Y. 1996. Evaluation of major and trace element XRF analyses using a flux to sample ratio of two to one glass beads. *Journal of Mineralogy, Petrology and Economic Geology,* 91, 62-72.

Lee, J.I. and Lee, Y.I. 1998. Feldspar albitization in Cretaceous non-marine mudrocks, Gyeongsang Basin, Korea. *Sedimentology,* 45, 745-754.

Lee, Y.I. and Jun, H.J., 1995. Diagenesis of Early Cretaceous Jangmokri Sandstone, Geoje Island, Korea. *Journal of the Geological Society of Korea,* 31, 32-46.

Nesbitt, H.W. and Young, G.M. 1982. Early Proterozoic climates and plate motions inferred from major element chemistry of lutites. *Nature,* 299, 715-717.

Nesbitt, H.W. and Young, G.M. 1984. Prediction of some weathering trends of plutonic and volcanic rocks based on thermodynamic and kinetic considerations. *Geochimica Cosmochimica Acta,* 48, 1523-1534.

Noh, J.H. and Park, H.S., 1990. Mineral diagenesis of sandstones from the Gyeongsang Supergroup in Goryeong area. *Journal of the Geological Society of Korea,* 26, 371-392.

Norrish, K. and Hutton, J.T. 1969. An accurate X-ray spectrographic method for the analysis of a wide range of geological samples. *Geochimica Cosmochimica Acta,* 33, 431-453.

Roser, B.P., Ishiga, H. and Lee, H.K., 2000. Geochemistry and provenance of Cretaceous sediments from the Euisong block, Gyeongsang Basin, Korea. In : Kumon, F. (Chief Editor) *Memoirs of the Geological Society of Japan,* (submitted).

Roser, B.P., Sawada, Y. and Kabeto, K. 1998. Crushing performance and contamination trials of a tungsten carbide ring mill compared to agate grinding. *Geoscience Reports of Shimane University,* 17, 1-9.

Son, J.-D. 1997. Cretaceous stratigraphy of Gyeongsang Basin. *Paleontological Society of Korea Special Publication,* 3, 31-46.

Yang, S.Y. and Chang, K.H. 1987. Mesozoic Erathem. In Lee, D.-S., ed., *Geology of Korea.* Seoul, Kyohak-Sa Publishing. Co., 157-201.

Yun, H., Moon, H.-S., Lee, H.K., Kim, I.-S. and Song, Y.-S. 1993. The color of the sedimentary rocks in the Euiseong Basin and its stratigraphical and paleoenvironmental implication. *Journal of the Paleontological Society of Korea,* 9, 93-114 (in Korean, English abstract).

(Received: 5 Nov. 1999, Accepted: 1 Dec. 1999)

（要　旨）

Barry Roser・石賀裕明・Hyun-Koo Lee・道前香緒里・山崎静子，1999，韓国慶尚累層群の義城ブロックの白亜系堆積岩類の主成分および微量成分分析，島根大学地球資源環境学研究報告，18, 1-10

韓半島には慶尚累層群の白亜系河川・湖成堆積岩が広く分布する．本論では主に亀尾・義城地域の義城ブロックに中の新洞および河陽層群 81 試料の砂岩・シルト岩・頁岩について全岩の蛍光 X 線分析結果を報告する．分析には CO_2，LOI と 11～16 の微量元素を含む．試料については地質学的位置づけ，岩石学的検討および元素組成の大まかな変化の概要も記述する．SiO_2 は鉱物の分級作用のため泥岩の～55wt%から砂岩の～85wt%まで変化に富む．多くの元素が Al_2O_3 と正の相関を示し，それらを含む鉱物が粘土鉱物と挙動をともにしていることを示す．Na_2O，CaO，Ba，Sr などの元素のグループは Al_2O_3 の増加とともに減少する．このことはこれらの元素が砂岩の試料では長石の中に存在しているか，または続成作用によって付加したことを示す．Zr は鉱物種のジルコンとして特徴的に存在するため，特定の濃集の傾向を示さない．重鉱物の濃集により，その他のいくつかの元素（Th, Ce, Ni, Cr および Y）などは高い濃度への分散を示す．より詳しい分析値の解釈は改めて報告する予定である．